ACS APPLIED MATERIALS & INTERFACES

Research Article

www.acsami.org

Guided in Situ Polymerization of MEH-PPV in Mesoporous Titania Photoanodes

Norma K. Minar, Pablo Docampo, Dina Fattakhova-Rohlfing, and Thomas Bein*

Department of Chemistry and Center for NanoScience (CeNS), University of Munich (LMU), Butenandtstrasse 5-13, 81377 Munich, Germany

Supporting Information

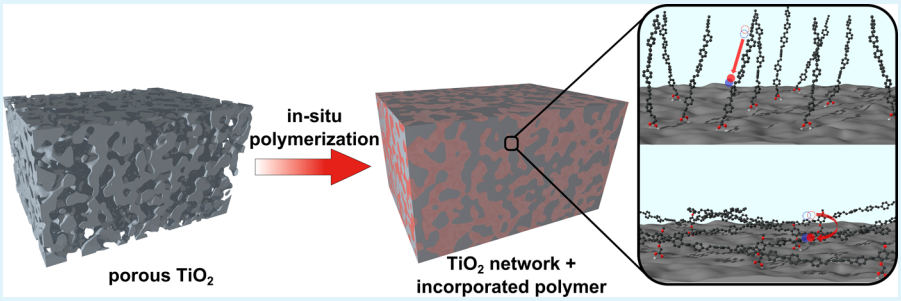

ABSTRACT: Incorporation of conjugated polymers into porous metal oxide networks is a challenging task, which is being pursued via many different approaches. We have developed the guided in situ polymerization of poly(2-methoxy-5-(2′-ethylhexyloxy)-*p*-phenylenevinylene) (MEH-PPV) in porous titania films by means of surface functionalization. The controlled polymerization via the Gilch route was induced by an alkoxide base and by increasing the temperature. The selected and specially designed surface-functionalizing linker molecules mimic the monomer or its activated form, respectively. In this way, we drastically enhanced the amount of MEH-PPV incorporated into the porous titania phase compared to nonfunctionalized samples by a factor of 6. Additionally, photovoltaic measurements were performed. The devices show shunting or series resistance limitations, depending on the surface functionalization prior to in situ polymerization of MEH-PPV. We suggest that the reason for this behavior can be found in the orientation of the grown polymer chains with respect to the titania surface. Therefore, the geometry of the anchoring via the linker molecules is relevant for exploiting the full electronic potential of the conjugated polymer in the resulting hybrid composite. This observation will help to design future synthesis methods for new hybrid materials from conjugated polymers and n-type semiconductors to take full advantage of favorable electronic interactions between the two phases.

KEYWORDS: *in situ polymerization, MEH-PPV, mesoporous titania, surface functionalization, nanocomposite, hybrid materials*

INTRODUCTION

Since their introduction by Heeger in the late 1970s, conducting polymers have inspired a wide range of research activities and applications.[1] The great appeal of this class of materials is the unusual combination of semiconductor and polymer properties. The advantages of polymeric materials—their potential low costs, low weight, good processability, and possible fine-tuning by organic synthesis—are coupled to the enormous diversity of electronic applications. In particular, poly(*p*-phenylenevinylene) (PPV) was discovered in 1990 as the first electroluminescent polymer[2] and has—together with its derivatives—emerged as a classical conjugated polymer used in polymer light-emitting diodes (PLEDs) and solar cells.[3,4] Especially, poly(2-methoxy-5-(2′-ethylhexyloxy)-*p*-phenylenevinylene) (MEH-PPV) has attracted much attention due to its relatively good solubility and easy processability.[5,6] The appeal for commercial applications of electroactive polymers such as MEH-PPV originates mainly from their solution processability, which includes advantageous methods such as inkjet and roll-to-roll printing, stamping, drop-casting, spin-coating, and dip-coating.[7] Nevertheless, the processing of a cast polymer film can be severely limited because most solvents will cause swelling, reorganization of the polymer chains, and even delamination.[8]

An interesting approach to overcome these stability issues is the covalent attachment of brushes of conjugated polymers onto surfaces. Polymer brushes in general are applied to tailor the interface and thus control surface properties such as wettability, biofouling resistance, adhesion, and stimuli responsiveness.[9] By anchoring conducting polymers such as MEH-PPV, the surface-related electronic properties of various materials can be tuned.[10−12] Through this approach, well-defined morphologies in heterojunction materials can in principle be constructed, resulting in controlled electronic

Received: February 9, 2015
Accepted: April 20, 2015
Published: April 20, 2015

DOI: 10.1021/acsami.5b01262
ACS Appl. Mater. Interfaces 2015, 7, 10356−10364

properties and enhanced interaction efficiencies between the two phases.[13,14]

Generally, there are two common methods for tethering polymer brushes: "grafting to" and "grafting from" approaches.[8] The grafting to method employs a preformed polymer with a reactive end group to attach the polymer chain to the surface. In contrast, in the grafting from approach polymer chains are grown directly from the surface. Several advantages of the grafting from strategy include a higher surface coverage, better suitability for high molecular weight polymers, and improved access to inner and outer surfaces of porous inorganic matrices.[8] The incorporation of polymers within nanostructured inorganic scaffolds opens up opportunities to engineer advanced materials with highly tunable features, such as mechanical, chemical, optical, and electrical properties.[15−20] Since the mid-1990s, there have been several attempts to integrate conjugated polymers into porous substrates by various polymerization techniques.[20−24] One elaborate way to efficiently introduce a conjugated polymer into a porous titania scaffold was shown by Zhang et al. for poly(3-hexyl)thiophene (P3HT).[25] In this approach, a surface functionalization of the porous material steered the growth of the P3HT onto the inner surface of the porous inorganic substrate. Employing this "grafting through" method, a larger surface coverage and consequently a more efficient photoinjection from the P3HT to the titania could be achieved compared to ex situ synthesized and infiltrated P3HT.[25]

Here we have, for the first time, adapted the surface functionalization approach for the MEH-PPV polymer and applied it to a mesoporous titania scaffold. The Gilch route was the synthesis route of choice for MEH-PPV because it is an inexpensive, nontoxic polymerization route initiated with an alkoxide base and by increasing the temperature.[26] The surface-functionalizing molecules were chosen and designed to mimic the monomer units. As a porous matrix we have used mesoporous titania films with a mean pore size of 20 nm, which are typically used in hybrid solar cells.[27,28]

Moreover, we have tested the applicability of this approach for incorporation of polymer into titania films with even smaller pores of around 10 nm.[29] The surface functionalization was monitored by reflection−absorption infrared spectroscopy (RAIR). The properties of the in situ polymerized MEH-PPV inside the mesoporous titania were characterized via UV−vis spectroscopy. Atomic force microscopy (AFM) and transmission electron microscopy (TEM) measurements provided information about the morphology of the porous titania films with the incorporated in situ polymerized MEH-PPV. Additionally, photovoltaic performance measurements provided data about the differing electronic properties depending on the functionalization.

EXPERIMENTAL SECTION

Materials. 2-Ethylhexyl bromide was purchased from Acros Organics and used as received. All other materials were purchased from Sigma-Aldrich Co. and used without further purification.

Methods. Reflection−absorption IR spectra were recorded with a BRUKER IFS 66v FTIR spectrometer. The sample chamber with a variable angle reflection accessory (A-513) was maintained at 2 mbar during the entire measurement by means of an Edwards rotary pump. In a typical measurement on silicon substrates, an angle of incidence of 54° to the surface normal was used. UV−vis measurements were performed on a Hitachi U3501 spectrophotometer equipped with an integrating sphere. Absorbance spectra were recorded in transmission geometry with plain glass or fluorine-doped tin oxide (FTO) coated glass as reference. Exposure to oxygen plasma was carried out with a Femto Plasma System from Diener Electronic typically operated at a power of 50 W and an oxygen flow of 4−5 cm^3(STP) min^{-1}. Gel-permeation chromatography (GPC) was performed on an Agilent 1200 Series machine equipped with a PSS SDV Lux precolumn (5 μ, 8.0 × 50 mm) followed by a PSS SDV Lux (1000 Å, 5 μ, 8.0 × 300 mm) column. Tetrahydrofuran (THF) was used as eluent with a flow rate of 1 mL min^{-1}. Atomic force microscopy (AFM) images were recorded with a Nanoink NSCRIPTOR DPN system in tapping mode. Transmission electron microscopy (TEM) was performed using a FEI Titan 80-300 instrument equipped with a field emission gun operated at 300 kV. Samples for TEM measurements were prepared by removing porous titania films with 20 nm pore size grafted with acrylic acid and subsequent in situ polymerization from the glass substrate and applied to a holey copper grid. For comparison a bare calcined porous titania film was investigated. Current−voltage characteristics were measured under simulated AM1.5G solar irradiation (Solar Light Model 16S) at 100 mW cm^{-2} in argon atmosphere. The light intensity was monitored with a Fraunhofer ISE-calibrated silicon reference cell equipped with a KG5 filter for reduced spectral mismatch. $J-V$ curves were recorded using a Keithley 2400 source meter. For liquid nuclear magnetic resonance (NMR) characterization of the observed signal multiplicities the following abbreviations were used: s (singlet), d (doublet), t (triplet), q (quartet), dd (doublet of a doublet), ddd (doublet of a doublet of a doublet), dt (doublet of triplet), tt (triplet of triplet), and m (multiplet).

*Synthesis of Monomer 1,4-Bis(bromomethyl)-2-(2-ethylhexyloxy)-5-methoxybenzene (**1**).* In a first step, 1-(2-ethylhexyloxy)-4-methoxybenzene was synthesized according to Anderson et al.[30] A detailed description of the synthesis can be found in the Supporting Information (SI). ^{1}H NMR (270 MHz, $CDCl_3$, TMS; ppm): δ 6.80 (s, 4H), 3.74 (d, J = 5.7 Hz, 2H), 3.73 (s, 3H), 1.66 (m, 1H), 1.21−1.52 (m, 8H), 0.82−0.90 (m, 6H). ^{13}C NMR (270 MHz, $CDCl_3$, TMS; ppm): δ 153.86, 115.68, 114.82, 71.47, 55.95, 39.71, 30.77, 29.34, 24.11, 23.30, 14.29, 11.32. Yield: 91%.

The bromomethylation of 1-(2-ethylhexyloxy)-4-methoxybenzene was conducted following a method described by Neef and Ferraris.[31] ***Warning!*** *The following reaction must be conducted in a well-ventilated fume hood. Mixtures of formaldehyde and hydrobromic acid can generate bromomethyl ethers which are likely to be human carcinogens.* ^{1}H NMR (270 MHz, $CDCl_3$, TMS; ppm): δ 6.86 (s, 4H), 4.52 (s, 4H), 3.87 (s, 5H), 0.8−1.8 (m, 15H). ^{13}C NMR (270 MHz, $CDCl_3$, TMS; ppm): δ 151.11, 151.05, 127.55, 127.41, 114.37, 113.84, 71.01, 56.32, 39.68, 30.71, 29.19, 28.76, 28.71, 24.10, 23.13, 14.18, 11.33. Yield: 78%. Overall yield: 71%.

*Synthesis of "Monomer Acid" ([2,5-Bis(bromomethyl)-4-methoxyphenoxy]acetic acid) **4**.* Similar to the synthesis of the monomer **1**, a carboxylated monomer was synthesized in a two-step protocol. First (4-methoxyphenoxy)acetic acid was synthesized according to a procedure described in the literature.[32] Yield: 66%.

In the second synthesis step, the (4-methoxyphenoxy)acetic acid was bromomethylated.[33] ^{1}H NMR (270 MHz, DMSO-d_6; ppm): δ 7.13 (s, 1H), 7.09 (s, 1H), 4.71 (s, 2H), 4.68 (s, 2H), 4.58 (s, 2H), 3.81 (s, 3H). ^{13}C NMR (270 MHz, DMSO-d_6, ppm): δ 170.63, 152.03, 150.06, 128.38, 127.53, 116.14, 114.61, 66.27, 56.68, 30.07. Yield: 57%. Overall yield: 38%.

Fabrication of Mesoporous Titania Films. *Mesoporous Titania: 10 nm Pore Size.* Mesoporous titania with an average pore size of 10 nm was synthesized according to the "brick and mortar" procedure developed in our group.[34] Titanium dioxide nanoparticles were prepared using a modified procedure developed by Niederberger et al.[35] Titanium tetrachloride (99.9%, 1.5 mL, 13.7 mmol) was dissolved in anhydrous toluene (10 mL) and added to benzyl alcohol (30 mL, 291 mmol) in a 100 mL Nalgene polycarbonate autoclave container under continuous stirring. The solution was kept at 60 °C for 20 h and then cooled to room temperature. The particles were separated by centrifugation at 50000 relative centrifugal force (rcf) for 30 min and used without further treatment. The centrifuged particles (without being subjected to washing procedures) contain about 45 wt % benzyl alcohol according to thermogravimetric analysis; this was

DOI: 10.1021/acsami.5b01262
ACS Appl. Mater. Interfaces 2015, 7, 10356−10364

taken into account for the adjustment of the TiO_2 content. To obtain a coating solution with 70 wt % TiO_2 nanoparticles and 30 wt % sol−gel titania precursors (based on the total Ti content in the final solution), a solution of Pluronic F127 (0.3 g, 0.02 mmol) in THF (4 mL) was added to centrifuged, unwashed particles (0.4 g, 2.2 mmol of TiO_2), ultrasonicated and stirred overnight until the particles were homogeneously re-dispersed. Subsequently, 0.4 mL (corresponding to 1.1 mmol TiO_2) of a prehydrolyzed sol−gel solution and 2.8 mL of THF was added (sol−gel solution; see later text), and the mixture was stirred for several minutes. The final solutions were transparent or translucent, being of a yellow to orange color. The sol−gel solution was prepared by adding hydrochloric acid (37%, 5.1 mL, 62.1 mmol) to tetraethyl orthotitanate (7.2 mL, 34.3 mmol) at room temperature in a 25 mL glass flask under continuous stirring for about 10 min. The films (around 380 nm thick) were prepared on FTO-coated glass (TEC-7 from Pilkington) by spin-coating (50−80 μL/(1 cm^2) substrate area) at 2000 rpm and calcined at 450 °C (0.9 °C min^{-1}) for 30 min.

Mesoporous Titania: 20 nm Pore Size. To synthesize mesoporous titania films with different thicknesses, the DSL 18 NR-T paste from dyesol was diluted with different amounts of ethanol. For a final thickness of around 1 μm 0.25 g of paste was diluted with 0.50 mL of ethanol. Thinner films with around 450 nm thickness were produced from a dilution of 0.25 g of paste with 0.80 mL of ethanol. The diluted paste was ultrasonicated for 2 h to ensure a colloidal mixing. The ethanol solution was spin-coated on different substrates (e.g., silicon, glass, fluorine-doped tin oxide) at 2000 rpm. All substrates were treated with oxygen plasma for 5 min beforehand. The resulting films were calcined at 450 °C for 30 min with a heating rate of 0.9 °C min^{-1}.

Functionalization of Titania Films. The calcined titania films were cleaned in oxygen plasma for 10 min. The surface of the cleaned mesoporous titania films was functionalized by immersing the films (three substrates with a 1.5 × 1.5 cm^2 film area each) in a 25 mM (16 mL) solution of the according linker molecule in dry acetone. The solution was refluxed at 70 °C for 3 h before the films were removed and rinsed with acetone and stored in the dark.

In Situ Polymerization of MEH-PPV. A 72 mg amount of monomer (0.17 mmol) was dissolved in dry THF (17 mL) and stirred under N_2 atmosphere in a 25 mL Schlenk tube to get a 10 mM solution. The titania films (three substrates with a 1.5 × 1.5 cm^2 film area each) were immersed in the solution without touching the walls of the vessel or disturbing the stirring bar. The reaction vessel was cooled to −80 °C under continuous stirring, and a suspension of 114 mg of potassium *tert*-butoxide in THF (2 mL) was added slowly through a septum. The cooling bath was removed after 30 min, and the reaction vessel was allowed to warm to room temperature. After 3 h stirring at room temperature the films were removed and rinsed with dry THF and methanol. Not-attached MEH-PPV was washed off with chlorobenzene, and the films were subsequently dried under vacuum for 1 h and kept in the dark.

Solar Cell Assembly. For photovoltaic measurements the mesoporous titania films were prepared on FTO substrates coated with a dense titania layer. The dense titania blocking layer was prepared by spin-coating 50 μL of a sol−gel solution at 4000 rpm on a patterned FTO substrate (2 × 1.5 cm^2). The titania sol−gel solution was produced by adding 0.75 mL (9 mmol) of concentrated hydrochloric acid to 1.05 mL (5 mmol) of tetraethyl orthotitanate and was further diluted with 15 mL of THF. After calcination at 450 °C for 30 min (0.9 °C min^{-1}) the mesoporous titania films were applied as mentioned earlier.

After functionalization and in situ polymerization as described previously a cover layer of MEH-PPV had to be applied to prevent contacting of the titania with the top electrode and this way short-circuiting of the devices. For this purpose, a solution of MEH-PPV (3 mg mL^{-1}, 150−250 kDa) in chlorobenzene was left soaking for 60 s on the mesoporous films (65 μL/(2.25 cm^2)), and afterward the films were spin-coated at 1000 rpm for 60 s.

After drying the films for 15 min at 120 °C under reduced pressure (2 × 10^{-2} mbar) a PEDOT:PSS layer was applied. A diluted PEDOT:PSS solution (2.5/1 = isopropanol/aqueous PEDOT:PSS) was left for 60 s on the substrates and then spin-coated at 1000 rpm for 60 s. The films were dried for 15 min at 110 °C under reduced pressure (2 × 10^{-2} mbar).

Silver electrodes, each of 100 nm thickness, were evaporated through a mask to yield an active area of 0.11 cm^2 for the final devices.

RESULTS AND DISCUSSION

Our approach of a guided in situ polymerization of MEH-PPV into mesoporous titania films was accomplished by grafting different functional molecules onto the surface of the titanium dioxide. The functionalization was intended to enable a targeted polymerization from the titania surface by participating in the process as the starting point of a growing polymer chain or as reaction partner of oligomers already formed in solution.[36] The selection of functional molecules was based on the polymerization mechanism of the applied Gilch route, which is schematically depicted in Figure 1A.[37] This approach is viewed

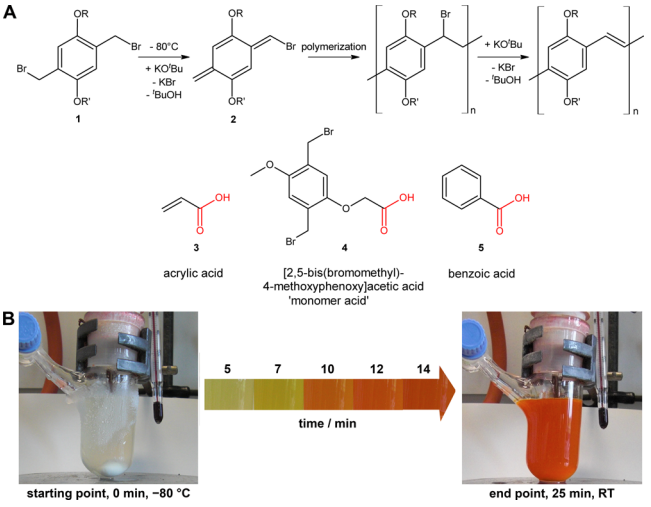

Figure 1. (A, top) Reaction scheme of the polymerization via the activated monomer **2**, a *p*-quinodimethane. R = CH_3, R′ = 2-ethyl(hexyl). (A, bottom) Selected molecules used for the functionalization of the titania surface. Carboxylic acid moieties acting as titania-specific anchor groups are depicted in red. (B) Illustration of the timeline of the thermally induced polymerization process.

as particularly interesting because it allows control of the polymer chain growth by tuning the reaction temperature. It is generally accepted that the active monomer for chain growth is α-halo-*p*-quinodimethane which results from an E2 elimination reaction of the monomer with the non-nucleophilic base potassium *tert*-butoxide.[38,39] Accordingly, the grafted functional molecules mimic either the monomer structure ("monomer acid", molecule **4**) or a part of the already activated monomer **2** (such as acrylic acid, molecule **3**) (see Figure 1A). Benzoic acid (**5**) was used as a reference molecule that cannot participate in the polymerization process and therefore cannot interfere with the chain growth of the MEH-PPV on the titania surface.

The successful functionalization of the mesoporous titania films was verified via RAIR spectroscopy, as shown in Figure 2. The strongest absorption at around 835 cm^{-1} corresponds to the inorganic Ti−O network (see SI Figure S1). Signals indicating aromatic moieties or carbon double bonds from the grafted molecules arise in the range from 1500 to 1600 cm^{-1}. The vibrational modes of the carboxyl groups can be seen in the spectra of the functionalized films around 1200, 1400, and 1725 cm^{-1}. Especially in the RAIR spectrum of the sample

DOI: 10.1021/acsami.5b01262
ACS Appl. Mater. Interfaces 2015, 7, 10356−10364

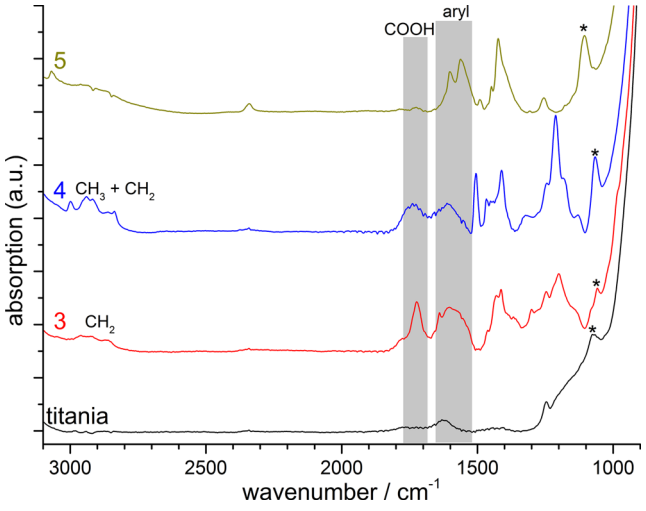

Figure 2. Reflection–absorption IR spectra of a nonfunctionalized titania film and films grafted with different carboxylic acids **3**–**5**. All spectra are normalized to the Ti–O signal at around 835 cm^{-1} (SI Figure S1). Signals marked with an asterisk correspond to the thin layer of SiO_2 of the silicon substrates underneath the titania films.

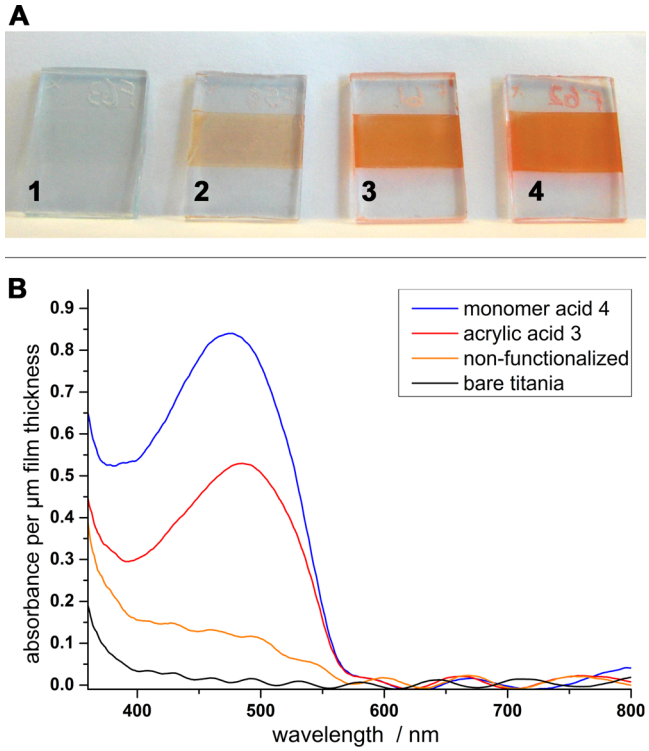

Figure 3. Effect of functionalization on in situ polymerization: (A) picture of mesoporous TiO_2 films (20 nm pore diameter) before polymerization (1; film thickness 1.5 μm) and after in situ polymerization [nonfunctionalized and in situ polymerized film (2, 1.5 μm thickness), acrylic acid functionalized and in situ polymerized films with the thickness of 1.5 (3), and 2 μm (4)]. All films are deposited on FTO-substrates. (B) Absorbance spectra of in situ polymerized titania films with different functionalization. The spectra are normalized to the film thickness.

grafted with monomer acid **4**, there are also peaks visible for C–H vibrations of the O–CH_3 and CH_2 groups around and below 3000 cm^{-1}.

The in situ polymerization of MEH-PPV within the mesoporous titania films is performed by immersing the samples vertically in a solution of 1,4-bis(bromomethyl)-2-(2-ethylhexyloxy)-5-methoxybenzene, monomer **1**, in THF. The reaction vessel was cooled to −80 °C, and then the base KOtBu was added. At this low temperature the monomer is fully converted into the activated form **2** (see Figure 1A).[26] This activated monomer can then react to a diradical induced by increasing the temperature, which is the starting point of the chain growth via a radical polymerization.[40] The progress of the polymerization reaction can be easily followed by the red shifting and increasing optical absorption of the reaction mixture, illustrated in Figure 1B. At the starting temperature of −80 °C, the solution of the monomer and the reactants is clear and colorless. Once the thermally induced polymerization sets off the increasing chain length of the resulting MEH-PPV, we observe a bathochromic shift in the absorption and the color of the reaction mixture changes gradually from light yellow to dark orange (see Figure 1B).[40] The pronounced effect of the surface functionalization on the amount of applicable MEH-PPV is already clearly visible by eye (see Figure 3A). Films that were grafted with acrylic acid **3** before the in situ polymerization are intensively orange in contrast to nonfunctionalized films which show only very light orange coloring. The functionalized and polymerized samples are homogeneously colored, which is remarkable considering the relatively thick porous titania layer of over 1.5 μm. In Figure 3B the corresponding UV–vis spectra of titania films with a pore size of 20 nm, typically used in dye-sensitized solar cells, are compared. The grafting of the titania surface with acrylic acid **3** or monomer acid **4** enhances the absorbance at 490 nm by a factor of 3.3 and 5.7 compared to nonfunctionalized and in situ polymerized samples, respectively.

One major question related to polymer chains grown from a surface is the influence of the confinement effects imposed by the substrate.[41] Therefore, in addition to the mesoporous titania films with a relatively large pore diameter of 20 nm we investigated the grafting and in situ polymerization method also with titania films with a smaller pore diameter of only 10 nm. Even with these small pores the absorbance after in situ polymerization of the functionalized titania surfaces is strongly enhanced compared to nonfunctionalized samples (SI Figure S2A).

To prove that the polymerization was indeed guided by the grafted molecules actively participating in the polymer chain growth, and not by other surface effects, we conducted two reference experiments. On the one hand, benzoic acid **5** was grafted onto the titania surface to change the polarity of the titania toward a more hydrophobic character without providing a polymerizable moiety. On the other hand, to ensure that the surface properties of titania were not affected by other conditions of the grafting process, such as prolonged refluxing, and thus promoted the in situ polymerization in some way, titania films were refluxed in plain acetone without any linker molecule ("No Linker"). After the in situ polymerization both samples—benzoic acid and No Linker—show only a low absorbance around 500 nm that is strikingly smaller compared to the acrylic acid grafting (cf. SI Figure S2A).

Another difference between the benzoic acid and the acrylic acid grafting is the strength of interaction of the MEH-PPV with the titania films, which was tested by thoroughly washing the in situ polymerized samples with chlorobenzene. After this washing step, samples functionalized with acrylic acid show a

DOI: 10.1021/acsami.5b01262
ACS Appl. Mater. Interfaces 2015, 7, 10356–10364

three times less reduced absorbance, and therefore less reduced amount of MEH-PPV, than benzoic acid grafted samples, as shown in Figure S2B, SI. This indicates that, in contrast to the benzoic acid grafted titania, most of the grown polymer chains in the acrylic acid functionalized films are covalently attached to the titania surface and/or remain inside the porous network and cannot be washed off. As expected, the change of the hydrophilic titania surface toward a hydrophobic surface—covered with benzyl groups—did not support the incorporation of the polymer.

Further information about the quality of the synthesized polymer, in the form of the HOMO−LUMO level energy gap E_g, can be extracted from the Tauc plots[42] of corresponding UV−vis data (see Figure 4 and SI Table S1). The value of the optical band gap E_g correlates with the conjugation length of the polymer. The latter relies on the overlap of the π-orbitals of the aromatic bonds, which in turn requires the phenyl rings and the vinyl bonds, i.e., the polymer backbone, to be reasonably coplanar.[43] The size of the energy gap E_g decreases with increasing conjugation length and saturates already at 20 monomer repeat units.[44,45]

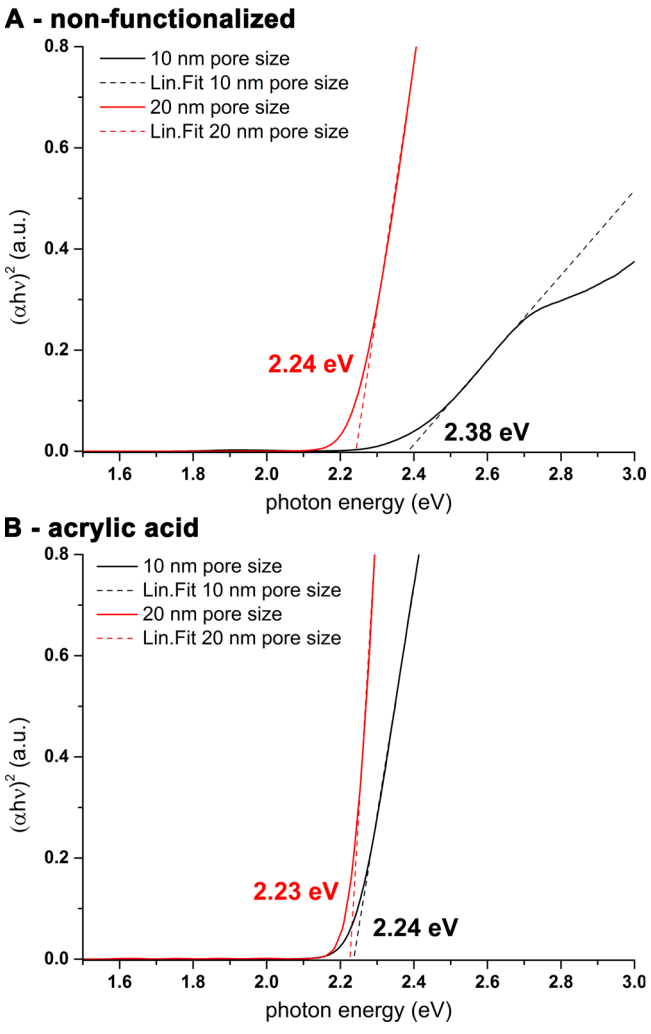

Figure 4. Tauc plots of mesoporous titania films with different pore sizes and without functionalization and in situ polymerization (A) and with acrylic acid grafting and in situ polymerization (B), respectively.

Many examples in the literature state that polymers synthesized in a confined space have a limited chain length and more defects compared to solution synthesized polymers, and therefore show a reduced conjugation length.[21,41,46−48] We made a similar observation for our systems. UV−vis measurements reveal that the commercially available MEH-PPV (40−70 kDa) and MEH-PPV synthesized in solution via the Gilch route exhibit a narrower optical band gap compared to the MEH-PPV synthesized inside the porous host (cf. SI Table S1). Moreover, in a size exclusion chromatography measurement the size of the MEH-PPV synthesized via the Gilch route was compared with the commercial sample of 40−70 kDa and showed an only slightly decreased chain length (SI Figure S3).

Juxtaposing the E_g values of MEH-PPV synthesized in titania with different pore diameters in Figure 4A and SI Table S1 gives a clear indication that the conjugation length is diminished for the smaller pore size. This seems to be counteracted by the functionalization of the titania surface with active molecules. This way the E_g value for acrylic acid functionalized films in the 10 nm pore system is similar to the value of MEH-PPV in nonfunctionalized 20 nm pore size titania (see Figure 4B). It appears that the functionalization in the smaller pores facilitates the polymerization and neutralizes limiting factors for the resulting conjugation length. Such a limitation does not seem to be substantial in the 20 nm pore size system, because the obtained E_g values are independent of the titania surface treatment (SI Table S1).

Although the optical band gap of the synthesized MEH-PPV is not affected by the functionalization in the bigger pore system, the UV−vis data show (cf. Figure 3 and SI Figure S2A) that the amount of polymer that is incorporated increases significantly, regardless of the titania pore size. The surface functionalization with active molecules such as acrylic acid **3** and monomer acid **4** seems to overcome the diffusion limitation and possibly enhances the chain growth inside the titania films. The total amount of conjugated photoactive polymer incorporated into the porous voids of the metal oxide semiconductor network is of special importance for hybrid bulk heterojunction devices.[49]

In hybrid solar cells based on titania and a conjugated polymer, excitons are created in the polymer phase upon photoexcitation and quenched at the titania interface after their diffusion toward the polymer/titania heterojunction.[50] A high interfacial area between these two phases is essential for a good charge transfer between the conjugated polymer and the titania film. This can be achieved through a high degree of pore filling of the nanostructured metal oxide with the conjugated polymer. Abrusci et al. showed that an optimum for an efficient polymer-based hybrid solar cell is reached at about 25% pore filling.[51] For example, in the case of monomer acid **4** functionalized films (20 nm pores), the absorption due to MEH-PPV obtained by in situ polymerization inside the pores (Figure 3B) is equivalent to a 125 nm thick dense film, assuming an extinction coefficient of around 1.5×10^5 cm^{-1}.[52] The film thickness measured by a profilometer was not increased after the polymerization, which implies that the synthesized polymer is located fully inside the pores, rather than being formed on the top of the titania network. This corresponds to a theoretical pore filling of around 25% assuming a porosity of 50% for the mesoporous films prepared from titania paste.[53] This conclusion is further supported by AFM measurements of titania films before and after grafting (monomer acid **4**) and subsequent in situ polymerization as shown in Figure 5. The surface of the bare titania film features sharp edges and crystal faces of the crystalline anatase particles (cf. Figure 5A). In

DOI: 10.1021/acsami.5b01262
ACS Appl. Mater. Interfaces 2015, 7, 10356−10364

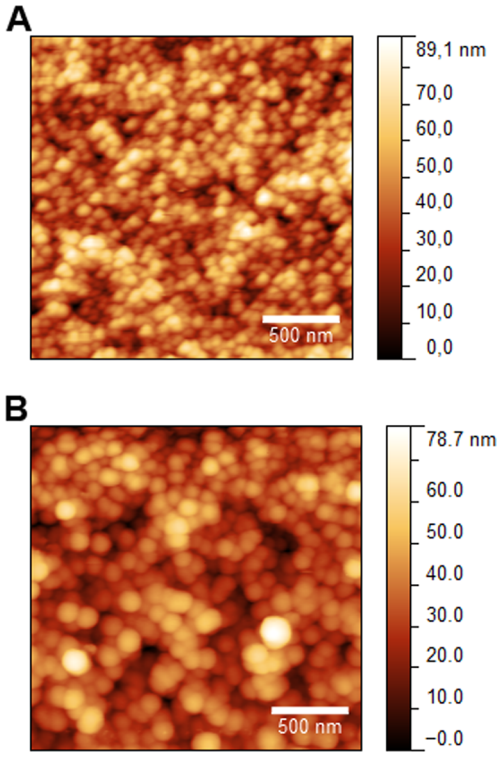

Figure 5. AFM measurements of differently treated titania films (20 nm pores, 20 nm anatase particles) in tapping mode: (A) bare calcined titania; (B) titania film after "monomer acid" functionalization and subsequent in situ polymerization.

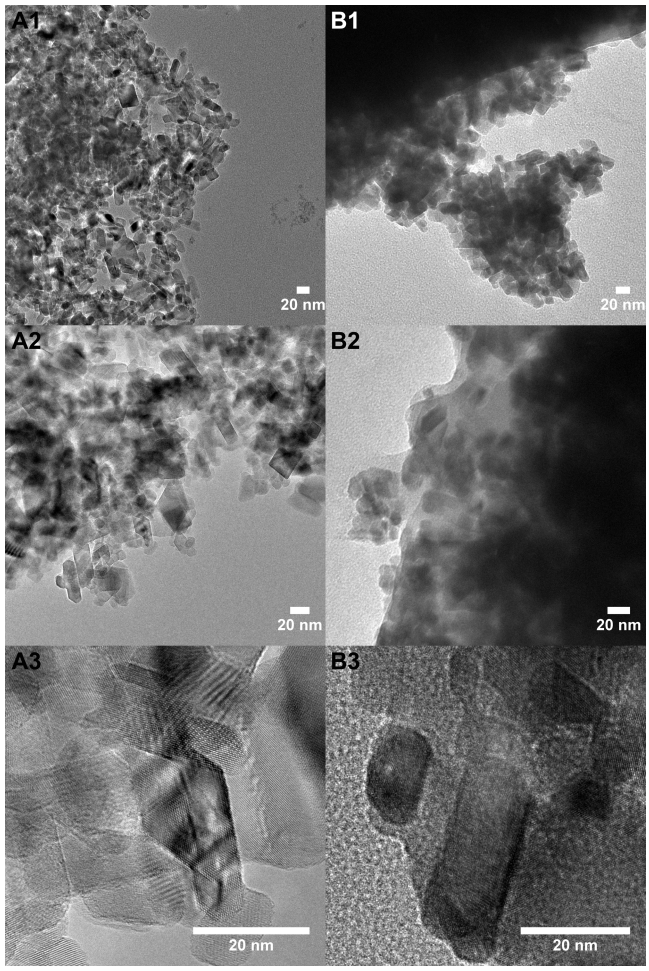

Figure 6. TEM micrograph of removed titania films of 1 μm thickness: (A1−A3) titania films after calcination; (B1−B3) titania films grafted with acrylic acid and after in situ polymerization.

contrast, the surface morphology of an MEH-PPV loaded film displays rounded smoothed features as shown in Figure 5B. This implies that the polymer completely covers the accessible surface of the anatase particles. The AFM image also shows that there is no closed polymer film on the surface and that the textural porosity is sustained.

To get better insights regarding the coverage of the titania surface with in situ synthesized polymer, TEM measurements of removed film material were performed. In the TEM micrographs in Figure 6B1−B3 the 20 nm anatase particles can be seen embedded in a layer of MEH-PPV. The accessible surface of the anatase particles seems to be fully covered with polymer, as shown in the AFM images in Figure 5B. In contrast, the TEM micrographs of bare, calcined titania films show the crystalline titania particles without any organic layer (see Figure 6A1−A3). The contrast of the inorganic oxide particles is clearer, and the lattice fringes of anatase are more prominent.

As already mentioned previously, conjugated polymers synthesized in a confined space are likely to show a diminished conjugation length and a higher defect density compared to samples synthesized in solution, which may result in reduced charge mobility.[36] In this context, in situ polymerized MEH-PPV inside porous titania films with 20 nm pores was further studied for applications in photovoltaic devices, as shown in Figure 7 (cf. SI Table S2).

Here, we can clearly observe three different regimes for the three studied systems. The performance of devices based on nonfunctionalized TiO_2 samples is clearly limited by shunting, as evidenced by the very low open circuit voltage. This could very likely be the result of incomplete surface coverage of MEH-PPV on the TiO_2 surface. This would result in a direct contact between the evaporated gold cathode and the exposed TiO_2 surface, which would result in a shorting path.[37]

Devices based on monomer acid **4** functionalized and in situ polymerized titania films, while showing the highest open circuit voltages, are clearly limited by series resistance losses.[38] These devices also exhibit the lowest short circuit currents, which is counterintuitive if we consider that these films show the highest light capture of the set. In contrast, the series resistance losses for devices based on acrylic acid **3** functionalized titania films are much lower than their monomer acid **4** counterparts, and also resulted in the highest photovoltaic performance of the set. To understand these differences, we consider the possible influence of the molecular structure of the surface linker on the growth of the polymer chains, which is schematically depicted in Figure S4, SI. We hypothesize that polymer growth seeded by the acrylic acid group results in polymer chains protruding more or less perpendicularly from the titania surface due to the geometry of the molecule, as depicted in SI Figure S4A. In the case of monomer acid **4** sensitized titania, there exist two nucleation points for the polymer growth on the side of the molecule. Here, we hypothesize that this results in polymer chain growth preferentially lying parallel to the surface of titania as shown in SI Figure S4B. Therefore, it is likely that the reduction in series resistance in acrylic acid **3** devices is the result of the

DOI: 10.1021/acsami.5b01262
ACS Appl. Mater. Interfaces 2015, 7, 10356−10364

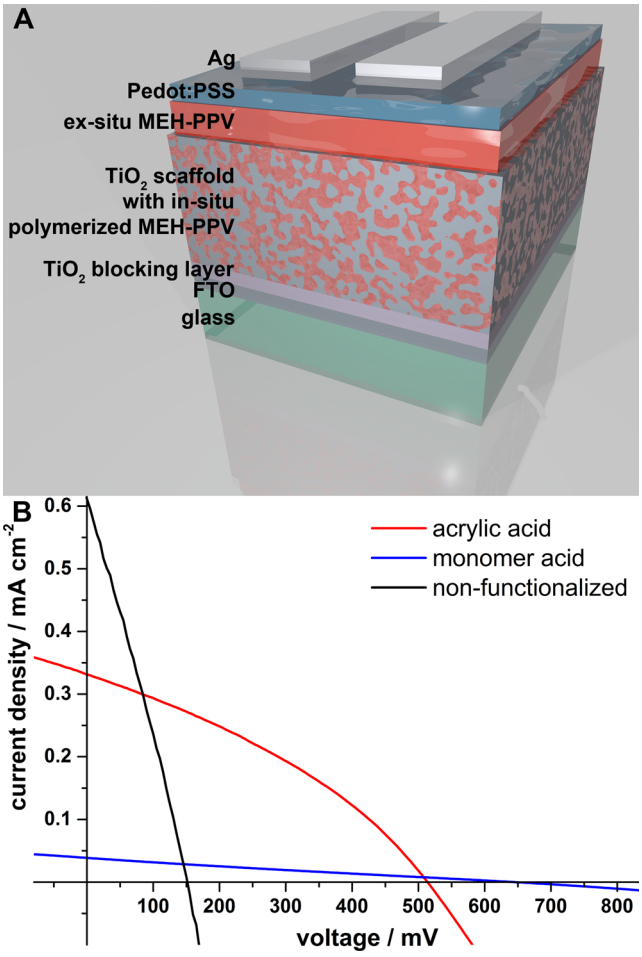

Figure 7. (A) Scheme of the device layout with the different layers. (B) *J*–*V* curves under AM 1.5 sunlight illumination of devices with functionalized and in situ polymerized titania films (black, no functionalization; blue, monomer acid; red, acrylic acid).

grown polymer chains directing photogenerated charges toward the titania surface via the more favorable transport along the conjugated polymer backbone.[54,55] For polymer chains not lying directly on the TiO_2 surface in the case of the monomer acid **4** functionalized devices, photogenerated charges would have to hop across different polymer chains to reach the titania surface, resulting in much slower charge transport and higher recombination rates,[56] thus explaining both the higher series resistance and the lower short circuit currents.

The surprising results with the different linker molecules show that for an efficient photovoltaic device high light absorbance is not sufficient and that the titania–polymer interface is crucial for charge separation and transport.

CONCLUSION

We have demonstrated the directed synthetic incorporation of MEH-PPV into mesoporous titanium dioxide films with more than a micrometer thickness. As the synthetic route we chose the Gilch route because it is an inexpensive, nontoxic polymerization initiated with an alkoxide base and by increasing the temperature.[26] The MEH-PPV polymerization within the titania structure was directed at reactive sites on the titania surface introduced via either acrylic acid or a "monomer acid" functionalization. This surface functionalization turned out to be essential for the incorporation of a large amount of the MEH-PPV into the titanium dioxide pores; it enhanced the amount of incorporated polymer up to nearly 6 times. Additionally, in the case of a smaller pore system (10 nm) the conjugation length—manifested in the E_g values—of the in situ synthesized MEH-PPV could be enhanced compared to nonfunctionalized samples. The performance of hybrid systems made with these two different anchor molecules in photovoltaic devices suggests that the orientation of the polymer chains with respect to the titania surface is essential for efficient power generation. This shows not only that it is important to fill the porous host with a maximum amount of polymer but also that it is important to tailor the nature of the linkage between the polymer and the titania which has a high impact on the electronic properties. On the one hand, the successful incorporation of a conjugated polymer into a porous metal oxide scaffold is therefore dependent on the functionalization of the surface with active linker molecules. On the other hand this alone is not sufficient to exploit the full electronic potential of the conjugated polymer in the resulting hybrid composite. Apparently, the surface anchoring geometry via the linker molecules is also very important, where a near-perpendicular orientation of the polymer chains with respect to the oxide surface seems to be advantageous. We anticipate that these insights into the electronic interactions between MEH-PPV and titania scaffolds depending on the polymer anchoring will help to develop new synthesis methods for more efficient hybrid materials.

ASSOCIATED CONTENT

Supporting Information

Detailed synthesis description of the monomer and linker molecules, RAIR spectra of functionalized titania films, UV–vis spectra of differently treated titania samples (10 nm pores) after in situ polymerization and rinsing with chlorobenzene, table of optical band gap values of MEH-PPV synthesized in the two porous titania systems with different surface functionalization, elution diagram of bulk MEH-PPV and a commercial MEH-PPV sample, table of the photovoltaic performance values, and figure of hypothesized orientation of in situ grown polymer chains. The Supporting Information is available free of charge on the ACS Publications website at DOI: 10.1021/acsami.5b01262.

AUTHOR INFORMATION

Corresponding Author

*E-mail: bein@lmu.de.

Author Contributions

N.K.M., D.F.-R., and T.B. conceived the experiments. N.K.M. performed the synthesis and characterization experiments. The manuscript was written through contributions of all authors. All authors have given approval to the final version of the manuscript.

Funding

Financial support from the Bavarian research network SolTech and from the Nanosystems Initiative Munich (NIM) funded by the DFG in Germany is gratefully acknowledged. We acknowledge support from the European Union through a Marie-Curie Intra-European Fellowship for P.D.

Notes

The authors declare no competing financial interest.

DOI: 10.1021/acsami.5b01262
ACS Appl. Mater. Interfaces 2015, 7, 10356–10364

■ ACKNOWLEDGMENTS

We thank Markus Döblinger for TEM measurements. We also thank Stephan Gleich, Sergio Januzzi, and Enrico Greul for sample preparation and Benjamin Mandlmeier and Johann M. Feckl for reading and commenting on the manuscript.

■ ABBREVIATIONS

AFM, atomic force microscopy
DMSO, dimethyl sulfoxide
FTO, fluorine-doped tin oxide
MEH-PPV, poly(2-methoxy-5-(2′-ethylhexyloxy)-*p*-phenylene vinylene)
P3HT, poly(3-hexylthiophen-2,5-diyl)
PEDOT:PSS, poly(3,4-ethylenedioxythiophene):poly(styrenesulfonate)
RAIR, reflection−absorption infrared
TEM, transmission electron microscopy
THF, tetrahydrofuran
TMS, trimethylsilane

■ REFERENCES

(1) Heeger, A. J. Nobel Lecture: Semiconducting and Metallic Polymers: The Fourth Generation of Polymeric Materials. *Rev. Mod. Phys.* **2001**, *73*, 681−700.
(2) Burroughes, J. H.; Bradley, D. D. C.; Brown, A. R.; Marks, R. N.; Mackay, K.; Friend, R. H.; Burns, P. L.; Holmes, A. B. Light-Emitting Diodes Based on Conjugated Polymers. *Nature* **1990**, *347*, 539−541.
(3) Brütting, W.; Buchwald, E.; Egerer, G.; Meier, M.; Zuleeg, K.; Schwoerer, M. Charge Carrier Injection and Transport in PPV Light Emitting Devices. *Synth. Met.* **1997**, *84*, 677−678.
(4) Benten, H.; Ogawa, M.; Ohkita, H.; Ito, S. Design of Multilayered Nanostructures and Donor−Acceptor Interfaces in Solution-Processed Thin-Film Organic Solar Cells. *Adv. Funct. Mater.* **2008**, *18*, 1563−1572.
(5) Lipomi, D. J.; Chiechi, R. C.; Reus, W. F.; Whitesides, G. M. Laterally Ordered Bulk Heterojunction of Conjugated Polymers: Nanoskiving a Jelly Roll. *Adv. Funct. Mater.* **2008**, *18*, 3469−3477.
(6) Chen, Z. K.; Pan, J. Q.; Xiao, Y.; Lee, N. H. S.; Chua, S. J.; Huang, W. Fully Soluble Poly(p-phenylenevinylene)s via Propagation Control of the Polymer Chain Conjugated Lengths. *Thin Solid Films* **2000**, *363*, 98−101.
(7) Kirchmeyer, S.; Starck, H. C. Polymer Electronics. Between Materials and Processes. *Nachr. Chem.* **2006**, *54*, 971−977.
(8) Azzaroni, O. Polymer Brushes Here, There, and Everywhere: Recent Advances in their Practical Applications and Emerging Opportunities in Multiple Research Fields. *J. Polym. Sci., Part A: Polym. Chem.* **2012**, *50*, 3225−3258.
(9) Stuart, M. A. C.; Huck, W. T. S.; Genzer, J.; Muller, M.; Ober, C.; Stamm, M.; Sukhorukov, G. B.; Szleifer, I.; Tsukruk, V. V.; Urban, M.; Winnik, F.; Zauscher, S.; Luzinov, I.; Minko, S. Emerging Applications of Stimuli-Responsive Polymer Materials. *Nat. Mater.* **2010**, *9*, 101−113.
(10) Kiriy, A.; Senkovskyy, V.; Sommer, M. Kumada Catalyst-Transfer Polycondensation: Mechanism, Opportunities, and Challenges. *Macromol. Rapid Commun.* **2011**, *32*, 1503−1517.
(11) Huddleston, N. E.; Sontag, S. K.; Bilbrey, J. A.; Sheppard, G. R.; Locklin, J. Palladium-Mediated Surface-Initiated Kumada Catalyst Polycondensation: A Facile Route Towards Oriented Conjugated Polymers. *Macromol. Rapid Commun.* **2012**, *33*, 2115−2120.
(12) Kang, S.; Ono, R. J.; Bielawski, C. W. Controlled Catalyst Transfer Polycondensation and Surface-Initiated Polymerization of a *p*-Phenyleneethynylene-Based Monomer. *J. Am. Chem. Soc.* **2013**, *135*, 4984−4987.
(13) Hains, A. W.; Ramanan, C.; Irwin, M. D.; Liu, J.; Wasielewski, M. R.; Marks, T. J. Designed Bithiophene-Based Interfacial Layer for High-Efficiency Bulk-Heterojunction Organic Photovoltaic Cells. Importance of Interfacial Energy Level Matching. *ACS Appl. Mater. Interfaces* **2009**, *2*, 175−185.
(14) Zhitenev, N. B.; SidorenkoA; Tennant, D. M.; Cirelli, R. A. Chemical Modification of the Electronic Conducting States in Polymer Nanodevices. *Nat. Nanotechnol.* **2007**, *2*, 237−242.
(15) Alexandre, M.; Dubois, P. Polymer-Layered Silicate Nanocomposites: Preparation, Properties and Uses of a New Class of Materials. *Mater. Sci. Eng. R* **2000**, *28*, 1−63.
(16) Laine, R. M.; Choi, J.; Lee, I. Organic−Inorganic Nanocomposites with Completely Defined Interfacial Interactions. *Adv. Mater.* **2001**, *13*, 800−803.
(17) Liang; Liu, J.; Gong, X. Thermosensitive Poly(*N*-isopropylacrylamide)−Clay Nanocomposites with Enhanced Temperature Response. *Langmuir* **2000**, *16*, 9895−9899.
(18) Pyun, J.; Matyjaszewski, K. Synthesis of Nanocomposite Organic/Inorganic Hybrid Materials Using Controlled/"Living" Radical Polymerization. *Chem. Mater.* **2001**, *13*, 3436−3448.
(19) Novak, B. M. Hybrid Nanocomposite Materials—Between Inorganic Glasses and Organic Polymers. *Adv. Mater.* **1993**, *5*, 422−433.
(20) Jing, C.; Chen, L.; Shi, Y.; Jin, X. Synthesis and Characterization of Exfoliated MEH-PPV/Clay Nanocomposites by in Situ Polymerization. *Eur. Polym. J.* **2005**, *41*, 2388−2394.
(21) Wu, C. G.; Bein, T. Conducting Polyaniline Filaments in a Mesoporous Channel Host. *Science* **1994**, *264*, 1757−1759.
(22) Tepavcevic, S.; Darling, S. B.; Dimitrijevic, N. M.; Rajh, T.; Sibener, S. J. Improved Hybrid Solar Cells via in Situ UV Polymerization. *Small* **2009**, *5*, 1776−1783.
(23) Kim, Y.; Lim, J.-w.; Sung, Y.-E.; Xia, J.-b.; Masaki, N.; Yanagida, S. Photoelectrochemical Oxidative Polymerization of Aniline and Its Application to Transparent TiO_2 Solar Cells. *J. Photochem. Photobiol., A* **2009**, *204*, 110−114.
(24) Alvaro, M.; Corma, A.; Ferrer, B.; Galletero, M. S.; García, H.; Peris, E. Increasing the Stability of Electroluminescent Phenylenevinylene Polymers by Encapsulation in Nanoporous Inorganic Materials. *Chem. Mater.* **2004**, *16*, 2142−2147.
(25) Zhang, Y.; Wang, C.; Rothberg, L.; Ng, M.-K. Surface-Initiated Growth of Conjugated Polymers for Functionalization of Electronically Active Nanoporous Networks: Synthesis, Structure and Optical Properties. *J. Mater. Chem.* **2006**, *16*, 3721−3725.
(26) Schwalm, T.; Rehahn, M. Toward Controlled Gilch Synthesis of Poly(*p*-phenylenevinylenes): Synthesis and Thermally Induced Polymerization of α-Bromo-*p*-quinodimethanes. *Macromolecules* **2007**, *40*, 3921−3928.
(27) O'Regan, B.; Gratzel, M. A Low-Cost, High-Efficiency Solar Cell Based on Dye-Sensitized Colloidal TiO_2 Films. *Nature* **1991**, *353*, 737−740.
(28) Ito, S.; Murakami, T. N.; Comte, P.; Liska, P.; Graetzel, C.; Nazeeruddin, M. K.; Graetzel, M. Fabrication of Thin Film Dye Sensitized Solar Cells with Solar to Electric Power Conversion Efficiency over 10%. *Thin Solid Films* **2008**, *516*, 4613−4619.
(29) Szeifert, J. M.; Fattakhova-Rohlfing, D.; Georgiadou, D.; Kalousek, V.; Rathousky, J.; Kuang, D.; Wenger, S.; Zakeeruddin, S. M.; Gratzel, M.; Bein, T. "Brick and Mortar" Strategy for the Formation of Highly Crystalline Mesoporous Titania Films from Nanocrystalline Building Blocks. *Chem. Mater.* **2009**, *21*, 1260−1265.
(30) Anderson, N.; Bagge, W.; Webber, C.; Zarras, P.; Davis, M. C. Procedure for the Rapid Synthesis of the Monomer 1,4-Bis-(chloromethyl)-2-(2-ethylhexyloxy)-5-methoxybenzene. *Synth. Commun.* **2008**, *38*, 3903−3908.
(31) Neef, C. J.; Ferraris, J. P. MEH-PPV: Improved Synthetic Procedure and Molecular Weight Control. *Macromolecules* **2000**, *33*, 2311−2314.
(32) Deffieux, D.; Fabre, I.; Courseille, C.; Quideau, S. Electrochemically-Induced Spirolactonization of α-(Methoxyphenoxy)-alkanoic Acids into Quinone Ketals. *J. Org. Chem.* **2002**, *67*, 4458−4465.
(33) Benjamin, I.; Hong, H.; Avny, Y.; Davidov, D.; Neumann, R. Poly(phenylenevinylene) Analogs with Ring Substituted Polar Side

DOI: 10.1021/acsami.5b01262
ACS Appl. Mater. Interfaces 2015, 7, 10356−10364

Chains and Their Use in the Formation of Hydrogen Bonding Based Self-Assembled Multilayers. *J. Mater. Chem.* **1998**, *8*, 919−924.
(34) Szeifert, J. M.; Fattakhova-Rohlfing, D.; Rathousky, J.; Bein, T. Multilayered High Surface Area "Brick and Mortar" Mesoporous Titania Films as Efficient Anodes in Dye-Sensitized Solar Cells. *Chem. Mater.* **2012**, *24*, 659−663.
(35) Niederberger, M.; Bartl, M. H.; Stucky, G. D. Benzyl Alcohol and Titanium Tetrachlorides—A Versatile Reaction System for the Nonaqueous and Low-Temperature Preparation of Crystalline and Luminescent Titania Nanoparticles. *Chem. Mater.* **2002**, *14*, 4364−4370.
(36) Lu, S.; Sun, S.-S.; Jiang, X.; Mao, J.; Li, T.; Wan, K. In Situ 3-Hexylthiophene Polymerization onto Surface of TiO_2 Based Hybrid Solar Cells. *J. Mater. Sci.: Mater. Electron.* **2010**, *21*, 682−686.
(37) Gilch, H. G.; Wheelwright, W. L. Polymerization of α-Halogenated *p*-Xylenes with Base. *J. Polym. Sci., Part A* **1966**, *4* (6), 1337−1349.
(38) Schwalm, T.; Wiesecke, J.; Immel, S.; Rehahn, M. Toward Controlled Gilch Synthesis of Poly(*p*-phenylene vinylenes): Anionic vs. Radical Chain Propagation, a Mechanistic Reinvestigation. *Macromolecules* **2007**, *40*, 8842−8854.
(39) Hontis, L.; Vrindts, V.; Vanderzande, D.; Lutsen, L. Verification of Radical and Anionic Polymerization Mechanisms in the Sulfinyl and the Gilch Route. *Macromolecules* **2003**, *36*, 3035−3044.
(40) Schwalm, T.; Wiesecke, J.; Immel, S.; Rehahn, M. The Gilch Synthesis of Poly(p-phenylene vinylenes): Mechanistic Knowledge in the Service of Advanced Materials. *Macromol. Rapid Commun.* **2009**, *30*, 1295−1322.
(41) Gorman, C. B.; Petrie, R. J.; Genzer, J. Effect of Substrate Geometry on Polymer Molecular Weight and Polydispersity during Surface-Initiated Polymerization. *Macromolecules* **2008**, *41*, 4856−4865.
(42) Tauc, J.; Grigorovici, R.; Vancu, A. Optical Properties and Electronic Structure of Amorphous Germanium. *Phys. Status Solidi B* **1966**, *15*, 627−637.
(43) Meier, H.; Stalmach, U.; Kolshorn, H. Effective Conjugation Length and UV/Vis Spectra of Oligomers. *Acta Polym.* **1997**, *48*, 379−384.
(44) Bredas, J. L.; Silbey, R.; Boudreaux, D. S.; Chance, R. R. Chain-Length Dependence of Electronic and Electrochemical Properties of Conjugated Systems: Polyacetylene, Polyphenylene, Polythiophene, and Polypyrrole. *J. Am. Chem. Soc.* **1983**, *105*, 6555−6559.
(45) Rissler, J. Effective Conjugation Length of π-Conjugated Systems. *Chem. Phys. Lett.* **2004**, *395*, 92−96.
(46) Scelta, D.; Ceppatelli, M.; Santoro, M.; Bini, R.; Gorelli, F. A.; Perucchi, A.; Mezouar, M.; van der Lee, A.; Haines, J. High Pressure Polymerization in a Confined Space: Conjugated Chain/Zeolite Nanocomposites. *Chem. Mater.* **2014**, *26*, 2249−2255.
(47) Wu, C.-G.; Bein, T. Conducting Carbon Wires in Ordered, Nanometer-Sized Channels. *Science* **1994**, *266*, 1013−1015.
(48) Pasetto, P.; Blas, H.; Audouin, F.; Boissiere, C.; Sanchez, C.; Save, M.; Charleux, B. Mechanistic Insight into Surface-Initiated Polymerization of Methyl Methacrylate and Styrene via ATRP from Ordered Mesoporous Silica Particles. *Macromolecules* **2009**, *42*, 5983−5995.
(49) Coakley, K. M.; Liu, Y.; McGehee, M. D.; Frindell, K. L.; Stucky, G. D. Infiltrating Semiconducting Polymers into Self-Assembled Mesoporous Titania Films for Photovoltaic Applications. *Adv. Funct. Mater.* **2003**, *13*, 301−306.
(50) Markov, D. E.; Tanase, C.; Blom, P. W. M.; Wildeman, J. Simultaneous Enhancement of Charge Transport and Exciton Diffusion in Poly(*p*-phenylene vinylene) Derivatives. *Phys. Rev. B* **2005**, *72*, No. 045217.
(51) Abrusci, A.; Ding, I. K.; Al-Hashimi, M.; Segal-Peretz, T.; McGehee, M. D.; Heeney, M.; Frey, G. L.; Snaith, H. J. Facile Infiltration of Semiconducting Polymer into Mesoporous Electrodes for Hybrid Solar Cells. *Energy Environ. Sci.* **2011**, *4*, 3051−3058.
(52) Gaudin, O. P. M.; Samuel, I. D. W.; Amriou, S.; Burn, P. L. Thickness Dependent Absorption Spectra in Conjugated Polymers: Morphology or Interference? *Appl. Phys. Lett.* **2010**, *96*, No. 053305.
(53) Docampo, P.; Hey, A.; Guldin, S.; Gunning, R.; Steiner, U.; Snaith, H. J. Pore Filling of Spiro-OMeTAD in Solid-State Dye-Sensitized Solar Cells Determined Via Optical Reflectometry. *Adv. Funct. Mater.* **2012**, *22*, 5010−5019.
(54) Nguyen, T.-Q.; Martini, I. B.; Liu, J.; Schwartz, B. J. Controlling Interchain Interactions in Conjugated Polymers: The Effects of Chain Morphology on Exciton−Exciton Annihilation and Aggregation in MEH−PPV Films. *J. Phys. Chem. B* **1999**, *104*, 237−255.
(55) Docampo, P.; Snaith, H. J. Obviating the Requirement for Oxygen in SnO_2-Based Solid-State Dye-Sensitized Solar Cells. *Nanotechnology* **2011**, *22*, 225403/1−225403/8.
(56) Garnett, E. C.; Yang, P. Silicon Nanowire Radial p−n Junction Solar Cells. *J. Am. Chem. Soc.* **2008**, *130*, 9224−9225.
(57) Noriega, R.; Rivnay, J.; Vandewal, K.; Koch, F. P. V.; Stingelin, N.; Smith, P.; Toney, M. F.; Salleo, A. A General Relationship Between Disorder, Aggregation and Charge Transport in Conjugated Polymers. *Nat. Mater.* **2013**, *12*, 1038−1044.
(58) Prins, P.; Grozema, F. C.; Schins, J. M.; Savenije, T. J.; Patil, S.; Scherf, U.; Siebbeles, L. D. A. Effect of Intermolecular Disorder on the Intrachain Charge Transport in Ladder-type Poly(*p*-phenylenes). *Phys. Rev. B* **2006**, *73*, No. 045204.
(59) Hertel, D.; Baessler, H. Photoconduction in Amorphous Organic Solids. *ChemPhysChem* **2008**, *9*, 666−688.

DOI: 10.1021/acsami.5b01262
ACS Appl. Mater. Interfaces 2015, 7, 10356−10364